

Receding Horizon Tracking Control of Wheeled Mobile Robots

Dongbing Gu and Huosheng Hu

Abstract—In this paper, a receding horizon (RH) controller is developed for tracking control of a nonholonomic mobile robot. The control stability is guaranteed by adding a terminal-state penalty to the cost function and constraining the terminal state to a terminal-state region. The stability analysis in the terminal-state region is investigated, and a virtual controller is found. The analysis results show that the RH tracking control has simultaneous tracking and regulation capability. Simulation results are provided to verify the proposed control strategy. It is shown that the control strategy is feasible.

Index Terms—Mobile robots, model predictive control (MPC), receding horizon (RH) control, tracking control.

I. INTRODUCTION

TRACKING control of nonholonomic mobile robots aims at controlling robots to track a given time varying trajectory (reference trajectory). It is a fundamental motion control problem and has been intensively investigated in the robotic community. One of the early research results of this problem [16] used a Lyapunov function to design a local asymptotic tracking controller. Global tracking was explored by dynamic feedback linearization techniques in [6], [9], and [24], backstepping techniques in [10], [13], and [15], and sliding mode techniques in [2]. Different time variant controllers or discontinuous controllers were developed [4], [21], [27]. These controllers require that linear or angular speeds must not converge to zero, i.e., reference trajectories are persistently excited. Therefore, they can not be used for the regulation problem of nonholonomic mobile robots. It is also difficult to constrain control signals in these controllers.

Recently, controllers with simultaneous tracking and regulation capability have been explored. A differential kinematic controller was developed in [8], which provides a global exponential stable property for both tracking control and regulation. A unifying framework for tracking control and regulation was presented in [20] by using dynamic feedback linearization. However, their controllers are not a single controller. The switching between controllers for tracking and regulation is required. In [18], a single global stable controller with simultaneous tracking and regulating capability was reported by using backstepping technique, and it also includes saturation constraints of control signals.

Receding Horizon (RH) or Model Predictive Control (MPC) is one of the frequently used optimization control techniques in industry. It is designed to handle optimization problems with constraints. It is an online optimization algorithm that predicts

system outputs based on current states and system model, finds an open loop control profile by numerical optimization, and applies the first control signal in the optimized control profile to the systems.

Due to the use of predictive control horizon in RH control, the control stability becomes one of the main problems [1]. It was shown that using infinite receding horizon can guarantee RH control stability for even nonlinear systems [17], but it is computational intractable in practice. For finite receding horizon, it was proved that forcing the terminal state to equal zero can guarantee the stability [23]. However, the terminal-state equality constraint is time consuming. Further work shows that the terminal-state equality constraint can be relaxed as a terminal-state inequality, i.e., a terminal-state region, by adding a terminal-state penalty to the optimized cost function if a linear state feedback controller exists in the terminal-state region [5], [7]. Furthermore, the linear feedback controller is never applied to the system since it is only used to find the terminal-state region to insure that the system will move into this region after finite control horizon. Recent work in [11], [19], [22], and [25] shows that the local linear feedback controller is not necessary. Any other controllers can be used in order to find the terminal-state region as long as a stability condition is met. And the work in [14] and [22] shows that the terminal-state penalty can be a control Lyapunov function that will guarantee the stability once the terminal state is within the terminal-state region.

Applying RH control to the regulation problem has been reported in [11] and [28]. The stability was not discussed in [28]. The terminal-state region in [11] is defined by a group of equations. This paper will develop an RH controller to achieve the tracking control of nonholonomic robots. First, the stability is guaranteed by adding a Lyapunov function to the cost function as the terminal-state penalty. A stability condition is found and used to find the terminal-state region and the corresponding controller. The terminal-state region becomes one of the optimization constraints in the RH algorithm. The terminal-state controller is never applied to control the robots. Second, the stabilizing RH controller is a single controller with simultaneous tracking and regulating capability. The switching between tracking control and regulation is not necessary. Third, control signal constraints are explicitly imposed on the controller. Finally, the proposed RH controller pursues a suboptimal solution in order to reduce the computation time. The main contribution of this paper is the development of the terminal-state region and the corresponding controller for simultaneously regulation and tracking of nonholonomic systems.

This paper is organized as follows. Section II introduces the tracking control problem of a nonholonomic mobile robot. The RH control scheme is described in Section III, including the stability analysis. The terminal-state controller and terminal-state region are found in Section IV. Section V explains the tracking

Manuscript received June 2, 2005. Manuscript received in final form January 10, 2006. Recommended by Associate Editor D. Prattichizzo.

The authors are with the Department of Computer Science, University of Essex, Colchester CO4 3SQ, U.K. (e-mail: dgu@essex.ac.uk).

Digital Object Identifier 10.1109/TCST.2006.872512

implementation. Simulation results are provided in Section VI. Finally, our conclusion and future works are discussed in Section VII.

II. KINEMATIC TRACKING CONTROL

A differential driving mobile robot is a typical nonholonomic mobile robot, which has two rear driving wheels and a front castor. The speed control of the two rear wheels (v_l and v_r) leads to the control of linear speed ($v = (v_l + v_r)/2$) and angular speed ($w = (v_l - v_r)/B$), where B is the wheelbase. The motion state of the robot can be described by its position (x, y) , the midpoint of the rear axis of the robot, and its orientation (θ) . The kinematics equation is as follows:

$$\dot{\mathbf{x}} = \begin{bmatrix} \dot{x} \\ \dot{y} \\ \dot{\theta} \end{bmatrix} = \begin{bmatrix} v \cos \theta \\ v \sin \theta \\ w \end{bmatrix} = \begin{bmatrix} \cos \theta & 0 \\ \sin \theta & 0 \\ 0 & 1 \end{bmatrix} \mathbf{u}. \quad (1)$$

The state and control signal vectors are denoted as $\mathbf{x} = (x, y, \theta)^T$ and $\mathbf{u} = (v, w)^T$.

The reference trajectories should also be described by a reference state vector $\mathbf{x}_r = (x_r, y_r, \theta_r)^T$ and a reference control signal vector $\mathbf{u}_r = (v_r, w_r)^T$ and have the same constraints as (1)

$$\dot{\mathbf{x}}_r = \begin{bmatrix} \dot{x}_r \\ \dot{y}_r \\ \dot{\theta}_r \end{bmatrix} = \begin{bmatrix} v_r \cos \theta_r \\ v_r \sin \theta_r \\ w_r \end{bmatrix} = \begin{bmatrix} \cos \theta_r & 0 \\ \sin \theta_r & 0 \\ 0 & 1 \end{bmatrix} \mathbf{u}_r. \quad (2)$$

To control (1) and to track (2), an error state \mathbf{x}_e can be defined as follows [16]:

$$\mathbf{x}_e = \begin{bmatrix} x_e \\ y_e \\ \theta_e \end{bmatrix} = \begin{bmatrix} \cos \theta & \sin \theta & 0 \\ -\sin \theta & \cos \theta & 0 \\ 0 & 0 & 1 \end{bmatrix} \begin{bmatrix} x_r - x \\ y_r - y \\ \theta_r - \theta \end{bmatrix}. \quad (3)$$

By using the error state and its dynamic model, the tracking control problem is converted into a regulation problem. The error state chosen in a rotated coordinate frame (3) can simplify the dynamic model. The error state dynamic model is derived as follows:

$$\begin{aligned} \dot{x}_e &= w y_e - v + v_r \cos \theta_e \\ \dot{y}_e &= -w x_e + v_r \sin \theta_e \\ \dot{\theta}_e &= w_r - w. \end{aligned} \quad (4)$$

Redefining the control signals

$$\mathbf{u}_e = \begin{bmatrix} u_1 \\ u_2 \end{bmatrix} = \begin{bmatrix} v_r \cos \theta_e - v \\ w_r - w \end{bmatrix}. \quad (5)$$

Then, the error state dynamic model (4) becomes

$$\dot{\mathbf{x}}_e = \begin{bmatrix} \dot{x}_e \\ \dot{y}_e \\ \dot{\theta}_e \end{bmatrix} = \begin{bmatrix} 0 & w & 0 \\ -w & 0 & 0 \\ 0 & 0 & 0 \end{bmatrix} \begin{bmatrix} x_e \\ y_e \\ \theta_e \end{bmatrix} + \begin{bmatrix} u_1 \\ v_r \sin \theta_e \\ u_2 \end{bmatrix}. \quad (6)$$

To analyze the local stability for the error state dynamic model (4), a linearized error state model of (6) can be obtained as follows:

$$\dot{\tilde{\mathbf{x}}}_e = \begin{bmatrix} 0 & w_r & 0 \\ -w_r & 0 & v_r \\ 0 & 0 & 0 \end{bmatrix} \tilde{\mathbf{x}}_e + \begin{bmatrix} 1 & 0 \\ 0 & 0 \\ 0 & 1 \end{bmatrix} \mathbf{u}_e. \quad (7)$$

Since the error state model (7) is controllable, local asymptotic stable controllers can be found [16]. However, the local linear controllable property is lost when the linear speed and angular speed converge to zero ($\lim_{t \rightarrow \infty} (v_r(t)^2 + w_r(t)^2) = 0$). Therefore, many controllers developed so far require this persistent excitation condition, i.e., the controlled robot cannot be stopped; otherwise, the stability will be lost.

Due to the requirement for the persistent excitation condition, the motion control of the nonholonomic mobile robots has been divided into two independent problems to handle: regulation (parking) and tracking. For the regulation problem ($\lim_{t \rightarrow \infty} (v_r(t)^2 + w_r(t)^2) = 0$), the local linearized model is not controllable, and therefore does not have a continuous time invariant feedback control law [3]. Instead, discontinuous control or smooth time-varying control can be found [12].

Independent controllers have been proposed for the two problems. The switching between two independent controllers is needed when the tracking robot is required to stop. The switching of controllers could lead to rapid changes of control signals, which in turn causes problems for system robustness. To avoid the switching, a single controller with simultaneous tracking and regulation capability is necessary [8], [18], [20].

III. STABILIZING RH CONTROL

A nonlinear nominal control system without considering any uncertainties, like (6), can be generally expressed as follows:

$$\dot{\mathbf{x}}_e(t) = \mathbf{f}(\mathbf{x}_e(t), \mathbf{u}_e(t)) \quad (8)$$

where $\mathbf{x}_e(t) \in R^n$ and $\mathbf{u}_e(t) \in R^m$ are the n dimensional state and m dimensional control vector, respectively. The function \mathbf{f} is assumed to be continuous. The tracking control is to find a suitable $\mathbf{u}_e(t)$ to drive the system (8) to move toward the equilibrium ($\mathbf{x}_e(t) = \mathbf{0}$ and $\mathbf{u}_e(t) = \mathbf{0}$). The constraints normally used are the control signal saturation constraints that can be expressed as follows:

$$\mathbf{u}_e(t) \in U$$

where $0 \in U \in R^m$ is a compact and convex set.

The goal of the tracking control is to minimize a given cost function as follows:

$$J(t, \mathbf{x}_e, \mathbf{u}_e) = \int_t^{t+T} L(\tau, \mathbf{x}_e(\tau), \mathbf{u}_e(\tau)) d\tau \quad (9)$$

where $L(\tau, \mathbf{x}_e(\tau), \mathbf{u}_e(\tau)) = \mathbf{x}_e(\tau)^T Q \mathbf{x}_e(\tau) + \mathbf{u}_e(\tau)^T R \mathbf{u}_e(\tau)$. Q and R are positive definite symmetric weight matrixes. T is the control horizon.

It is well known that the controller found in (9) is not guaranteed to be stable due to the use of a finite receding horizon [1]. The RH stability can be guaranteed by adding a terminal-state penalty term to the cost function and a terminal-state constraint to the optimization in the RH controller [5], [19]. The cost function for the tracking problem is changed as follows:

$$J(t, \mathbf{x}_e(t), \mathbf{u}_e(t)) = g(\mathbf{x}_e(t+T)) + \int_t^{t+T} L(\tau, \mathbf{x}_e(\tau), \mathbf{u}_e(\tau)) d\tau \quad (10)$$

where $g(\mathbf{x}_e(t+T))$ is the terminal state penalty and is assumed to be a continuous, differentiable function, $g(\mathbf{0}) = 0$, and $g(\mathbf{x}_e(t)) > 0$ for all $\mathbf{x}_e(t) \neq \mathbf{0}$.

At time t , the open loop optimization problem (OP) in the RH control framework to be solved online can be formulated as follows:

$$\begin{aligned} \min_{\mathbf{u}_e} \quad & J(t, \mathbf{x}_e(t), \mathbf{u}_e(t)) \quad (11) \\ \text{subject to:} \quad & \dot{\mathbf{x}}_e(\tau) = \mathbf{f}(\mathbf{x}_e(\tau), \mathbf{u}_e(\tau)) \\ & \mathbf{x}_e(\tau) \in U \quad (\tau \in [t, t+T]) \\ & \mathbf{x}_e(t+T) \in \Omega \quad (12) \end{aligned}$$

where Ω is the terminal-state region.

Our RH control algorithm can be described as follows.

- 1) The current error state $\mathbf{x}_e(\tau)$ is fed back. Based on this feedback state, an open loop optimal control function $\bar{\mathbf{u}}_e(\tau, \mathbf{x}_e(t))$ can be found by solving the OP (11) and (12) for the period $t \leq \tau \leq t+T$. The open loop control function $\bar{\mathbf{u}}_e(\tau, \mathbf{x}_e(t))$ defines a state trajectory $\bar{\mathbf{x}}_e(\tau)$, and both of them depend on the current state $\mathbf{x}_e(t)$.
- 2) The RH control only uses $\bar{\mathbf{u}}_e(\tau, \mathbf{x}_e(t))$ to control the system (8) over a period $[t, t+\delta)$ ($\delta < T$). Therefore, the RH control function $\mathbf{u}_e(\tau)$ and the corresponding state trajectory $\mathbf{x}_e(\tau)$ also depend on the current error state $\mathbf{x}_e(\tau)$ and are expressed as follows:

$$\begin{aligned} \mathbf{u}_e(\tau, \mathbf{x}_e(t)) &= \bar{\mathbf{u}}_e(\tau, \mathbf{x}_e(t)) \quad \tau \in [t, t+\delta) \\ \mathbf{x}_e(\tau) &= \bar{\mathbf{x}}_e(\tau). \quad (13) \end{aligned}$$

- 3) At time $t+\delta$, the RH control needs to read the error state $\mathbf{x}_e(t+\delta)$ and solve the OP again. A terminal-state controller $\mathbf{u}_e^L(\tau, \mathbf{x}_e(t+\delta))$ for the terminal-state region Ω is found first. Then, a feasible control function $\hat{\mathbf{u}}_e(\tau, \mathbf{x}_e(t+\delta))$ is constructed based on $\bar{\mathbf{u}}_e(\tau, \mathbf{x}_e(t+\delta))$ and the terminal-state controller $\mathbf{u}_e^L(\tau, \mathbf{x}_e(t+\delta))$

$$\hat{\mathbf{u}}_e(\tau, \mathbf{x}_e(t+\delta)) = \begin{cases} \bar{\mathbf{u}}_e(\tau, \mathbf{x}_e(t+\delta)), & \text{if } t+\delta \leq \tau \leq t+T \\ \mathbf{u}_e^L(\tau, \mathbf{x}_e(t+\delta)), & \text{if } t+T \leq \tau \leq t+T+\delta. \end{cases} \quad (14)$$

This constructed control function $\hat{\mathbf{u}}_e(\tau, \mathbf{x}_e(t+\delta))$ is used as an initial solution to the OP for the period $t+\delta \leq \tau \leq t+T+\delta$. After solving the OP at time $t+\delta$, an open loop optimal control function $\bar{\mathbf{u}}_e(\tau, \mathbf{x}_e(t+\delta))$ is obtained again, which depends on the current state $\mathbf{x}_e(t+\delta)$. The RH control function is obtained by using $\mathbf{u}_e(\tau, \mathbf{x}_e(t+\delta)) = \bar{\mathbf{u}}_e(\tau, \mathbf{x}_e(t+\delta))$ for the period $[t+\delta, t+2\delta)$.

- 4) This procedure will continue until the control achieves a satisfying performance.

Stability Theorem: Suppose the reference control signals are bounded, i.e., $\sup_{t \geq 0} v_r(t) < v_{\max}$, $\sup_{t \geq 0} w_r(t) < w_{\max}$, and the OP is feasible at the time $t=0$. The RH control algorithm described previously for the system (8) is asymptotically stable if a terminal-state controller $\mathbf{u}_e^L(t)$ exists such that the following condition is satisfied:

$$\dot{g}(\mathbf{x}_e(t)) + L(t, \mathbf{x}_e(t), \mathbf{u}_e(t)) \leq 0 \quad (15)$$

for any state $\mathbf{x}_e(t)$ belonging to the terminal region Ω .

Proof: Let $\bar{V}(t, \bar{\mathbf{x}}_e(t))$ denote the OP value function and $V(t, \mathbf{x}_e(t))$ the RH value function. We need to prove that $V(t, \mathbf{x}_e(t))$ is nonincreasing and in turn implies the system (8) is asymptotically stable $\mathbf{x}_e(t) \rightarrow 0$ as $t \rightarrow \infty$.

For a time period $\tau \in [t, t+\delta)$, the RH value function $V(t, \mathbf{x}_e(t))$ is nonincreasing due to the following equation:

$$\begin{aligned} V(\tau, \mathbf{x}_e(t)) &= \bar{V}(\tau, \bar{\mathbf{x}}_e(t)) \\ &= \bar{V}(t, \bar{\mathbf{x}}_e(t)) - \int_t^{\tau} L(s, \bar{\mathbf{x}}_e(s), \bar{\mathbf{u}}_e(s)) ds \\ &= V(t, \mathbf{x}_e(t)) - \int_t^{\tau} L(s, \mathbf{x}_e(s), \mathbf{u}_e(s)) ds \\ &\leq V(t, \mathbf{x}_e(t)). \quad (16) \end{aligned}$$

For the time instant $t+\delta$, the OP value function has the following result:

$$\bar{V}(t+\delta, \hat{\mathbf{x}}_e(t+\delta)) \geq \bar{V}(t+\delta, \bar{\mathbf{x}}_e(t+\delta)) \quad (17)$$

where $\hat{\mathbf{x}}_e(t+\delta)$ is the state trajectory when using the control function $\hat{\mathbf{u}}_e(t+\delta, \mathbf{x}_e(t+\delta))$ (14), and $\bar{V}(t+\delta, \hat{\mathbf{x}}_e(t+\delta))$ is the corresponding OP value function.

We know

$$\bar{V}(t+\delta, \bar{\mathbf{x}}_e(t+\delta)) = V(t+\delta, \mathbf{x}_e(t+\delta)). \quad (18)$$

We can have the following result for two time instants t and $t+\delta$:

$$\begin{aligned} & \bar{V}(t+\delta, \hat{\mathbf{x}}_e(t+\delta)) - V(t, \mathbf{x}_e(t)) \\ &= g(\hat{\mathbf{x}}_e(t+T+\delta)) + \int_{t+\delta}^{t+T+\delta} L(s, \hat{\mathbf{x}}_e(s), \hat{\mathbf{u}}_e(s)) ds \\ & \quad - g(t, \bar{\mathbf{x}}_e(t+T)) - \int_t^{t+T} L(s, \bar{\mathbf{x}}_e(s), \bar{\mathbf{u}}_e(s)) ds \\ &= g(\hat{\mathbf{x}}_e(t+T+\delta)) - g(t, \bar{\mathbf{x}}_e(t+T)) \\ & \quad + \int_{t+T}^{t+T+\delta} L(s, \hat{\mathbf{x}}_e(s), \hat{\mathbf{u}}_e(s)) ds \\ & \quad - \int_t^{t+\delta} L(s, \bar{\mathbf{x}}_e(s), \bar{\mathbf{u}}_e(s)) ds. \quad (19) \end{aligned}$$

By integrating (15), we have

$$\begin{aligned} & g(\hat{\mathbf{x}}_e(t+T+\delta)) - g(\hat{\mathbf{x}}_e(t+T)) \\ & \quad + \int_{t+T}^{t+T+\delta} L(s, \hat{\mathbf{x}}_e(s), \hat{\mathbf{u}}_e(s)) ds \leq 0. \quad (20) \end{aligned}$$

At time instant $t + T$, we know $\hat{\mathbf{x}}_e(t + T) = \bar{\mathbf{x}}_e(t + T)$ due to the constructed control (14). So the following result can be obtained from (19):

$$\begin{aligned} & \bar{V}(t + \delta, \hat{\mathbf{x}}_e(t + \delta)) - V(t, \mathbf{x}_e(t)) \\ & \leq - \int_t^{t+\delta} L(s, \bar{\mathbf{x}}_e(s), \bar{\mathbf{u}}_e(s)) ds \\ & = - \int_t^{t+\delta} L(s, \mathbf{x}_e(s), \mathbf{u}_e(s)) ds. \end{aligned} \quad (21)$$

Finally, using (17), (18), and (21), we have

$$\begin{aligned} & V(t + \delta, \mathbf{x}_e(t + \delta)) - V(t, \mathbf{x}_e(t)) \\ & \leq - \int_t^{t+\delta} L(s, \mathbf{x}_e(s), \mathbf{u}_e(s)) ds \\ & \leq 0. \end{aligned} \quad (22)$$

Repeatedly using the inequality (22) yields

$$\begin{aligned} & V(t, \mathbf{x}_e(t)) - V(0, \mathbf{x}_e(0)) \\ & \leq - \int_0^t L(s, \mathbf{x}_e(s), \mathbf{u}_e(s)) ds \\ & = - \int_0^t (\mathbf{x}_e(s)^T Q \mathbf{x}_e(s) + \mathbf{u}_e(s)^T R \mathbf{u}_e(s)) ds \\ & \leq - \int_0^t \mathbf{x}_e(s)^T Q \mathbf{x}_e(s) ds. \end{aligned} \quad (23)$$

Now we can say the RH value function $V(t, \mathbf{x}_e(t))$ is nonincreasing and bounded below by zero. This implies the integral term in the right side of the inequality (23) is low bounded.

To guarantee $\mathbf{x}_e(t)$ is bounded, it can be seen from (4) that the reference speeds have to be bounded, i.e., $\sup_{t \geq 0} v_r(t) < v_{\max}$ and $\sup_{t \geq 0} w_r(t) < w_{\max}$. $\dot{\mathbf{x}}_e(t)$ is bounded from the properties of \mathbf{f} . According to Barbalat's lemma [26], this means $\mathbf{x}_e(t)^T Q \mathbf{x}_e(t) \rightarrow 0$ as $t \rightarrow \infty$. When we take $Q > 0$, the system is asymptotically stable, i.e., $\mathbf{x}_e(t) \rightarrow 0$ as $t \rightarrow \infty$. \square

It should be noted that the proved stability does not necessarily depend on the optimality of the cost function. We can build up a suboptimal RH control algorithm by using a suboptimal solution or feasible solution $\tilde{\mathbf{u}}(\tau, \mathbf{q}(t + \delta))$ to the OP rather than its optimal solution $\bar{\mathbf{u}}(\tau, \mathbf{q}(t + \delta))$ in step 3) of the RH control algorithm.

IV. TERMINAL-STATE REGION AND ITS CONTROLLER

A Lyapunov function for the terminal-state penalty can be defined as follows:

$$g(\mathbf{x}_e(t + T)) = \frac{1}{2} \mathbf{x}_e(t + T)^T \mathbf{x}_e(t + T). \quad (24)$$

The positive definite weight matrixes of the L function in (9) are selected as follows:

$$Q = \begin{bmatrix} q_{11} & 0 & 0 \\ 0 & q_{22} & 0 \\ 0 & 0 & q_{33} \end{bmatrix}, \quad R = \begin{bmatrix} r_{11} & 0 \\ 0 & r_{22} \end{bmatrix} \quad (25)$$

where ($q_{11} > 0, q_{22} > 0, q_{33} > 0$) and ($r_{11} \geq 0, r_{22} \geq 0$). Then, stability condition (15) becomes

$$\begin{aligned} & \dot{g}(\mathbf{x}_e(t + T)) + L(t + T) \\ & = x_{eT} \dot{x}_{eT} + y_{eT} \dot{y}_{eT} + \theta_{eT} \dot{\theta}_{eT} + L(t + T) \\ & = -x_{eT} u_1^L + y_{eT} v_r \sin \theta_{eT} + u_2^L \theta_{eT} + L(t + T) \\ & = -x_{eT} u_1^L + y_{eT} v_r \sin \theta_{eT} + u_2^L \theta_{eT} \\ & \quad + q_{11} x_{eT}^2 + q_{22} y_{eT}^2 + q_{33} \theta_{eT}^2 + r_{11} u_1^{L^2} + r_{22} u_2^{L^2} \end{aligned} \quad (26)$$

where the subscript T denotes the terminal state. The terminal-state feedback controller can be selected as follows:

$$\begin{aligned} u_1^L &= \alpha x_{eT} \\ u_2^L &= -\beta \theta_{eT} \end{aligned} \quad (27)$$

where $\alpha \geq 0$ and $\beta \geq 0$. The stability condition (15) is changed to

$$\begin{aligned} & \dot{g}(\mathbf{x}_e(t + T)) + L(t + T) \\ & = -(\alpha - q_{11} - r_{11} \alpha^2) x_{eT}^2 - (\beta - q_{33} - r_{22} \beta^2) \theta_{eT}^2 \\ & \quad + y_{eT} v_r \sin \theta_{eT} + q_{22} y_{eT}^2. \end{aligned} \quad (28)$$

To have a negative derivative of the value function, the following requirement for the weight parameters is required:

$$\begin{aligned} \alpha - q_{11} - r_{11} \alpha^2 &\geq q_{22} \\ \beta - q_{33} - r_{22} \beta^2 &\geq 0 \end{aligned} \quad (29)$$

and the terminal-state region is defined as follows:

$$\begin{aligned} |x_{eT}| &\geq |y_{eT}| \\ y_{eT} \theta_{eT} &< 0. \end{aligned} \quad (30)$$

In summary, the terminal-state controller will be defined by (27), the cost function weights will be constrained by (29), and the terminal-state region will be defined by (30).

Furthermore, the control signal region also limits the terminal-state region Ω . The following control signal constraints are used in this paper:

$$\begin{aligned} 0 &\leq v \leq v_{\max} \\ -w_{\max} &\leq w \leq w_{\max}. \end{aligned} \quad (31)$$

From (5), (27), and (31), the terminal state should be further constrained by the control signal region

$$\begin{aligned} \frac{(v_r \cos \theta_{eT} - v_{\max})}{\alpha} &\leq x_{eT} \leq \frac{(v_r \cos \theta_{eT} + v_{\max})}{\alpha} \\ -\frac{(w_{\max} + w_r)}{\beta} &\leq \theta_{eT} \leq \frac{(w_{\max} - w_r)}{\beta}. \end{aligned} \quad (32)$$

An additional requirement identified from (28) is that the reference linear speed is nonnegative ($v_r \geq 0$).

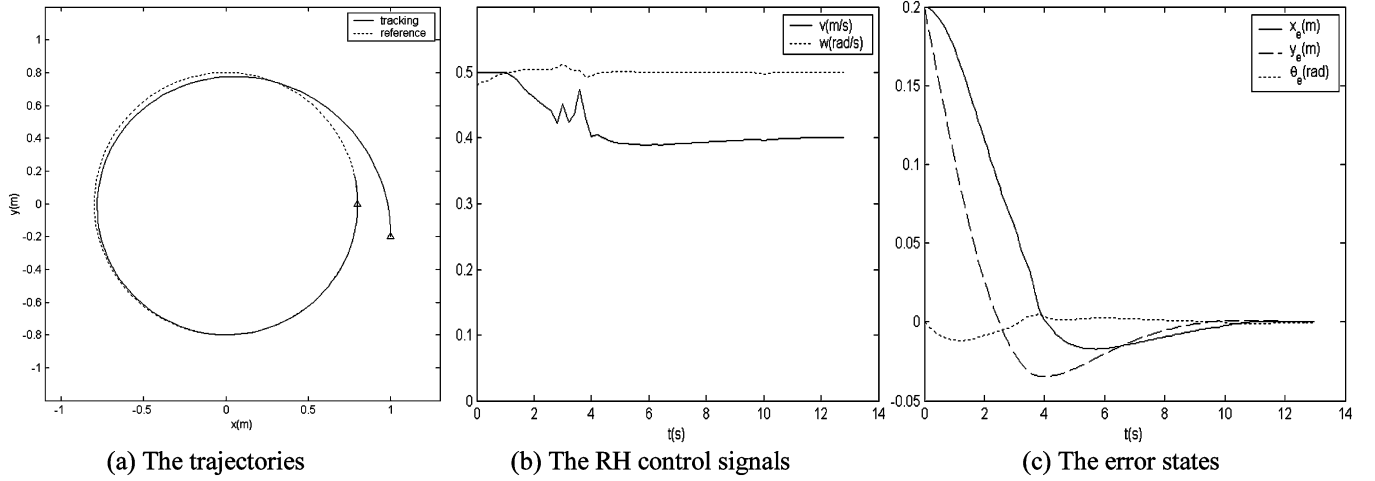


Fig. 1. Circle tracking.

V. IMPLEMENTATION

The first reference trajectory in the tests is a circle defined as follows:

$$\begin{aligned} x_r &= 0.8 \cos(0.5t) \\ y_r &= 0.8 \sin(0.5t). \end{aligned}$$

The second reference trajectory is an eight-shaped trajectory adopted in [20]

$$\begin{aligned} x_r &= \sin\left(\frac{t}{10}\right) \\ y_r &= \sin\left(\frac{t}{20}\right). \end{aligned}$$

The eight-shaped trajectory is a persistently excited trajectory and has sharp changes in its reference speeds. The third reference trajectory is a parallel parking line adopted in [18]. It is not a persistently excited trajectory and will stop at the final position

$$\begin{aligned} x_r &= \begin{cases} 0.8 \cos\left(0.1t + \frac{\pi}{4}\right), & 0 \leq t < 5\pi \\ -0.4\sqrt{2}, & t \geq 5\pi \end{cases} \\ y_r &= \begin{cases} 0.4 \sin\left(0.2t + \frac{\pi}{2}\right), & 0 \leq t < 5\pi \\ -0.4, & t \geq 5\pi. \end{cases} \end{aligned}$$

The weight parameters of the RH controller can affect the tracking performances. For the persistent excitation trajectories (circle and eight-shaped curve), the parameters are selected as follows:

$$\begin{aligned} q_{11} = q_{22} = q_{33} &= 0.5, & q_{11} = q_{22} &= 0.2 \\ \alpha &= 2, & \beta &= 1. \end{aligned}$$

For the parallel parking, the parameters are selected as follows to avoid slow convergence:

$$\begin{aligned} q_{11} &= 0.5, & q_{22} &= 1, & q_{33} &= 0.1, & q_{11} = q_{22} &= 0.1 \\ \alpha &= 2, & \beta &= 1. \end{aligned}$$

The control signal constraints for the circle and the parallel parking line are selected as follows:

$$\begin{aligned} v_{\max} &= 0.5 \left(\frac{\text{m}}{\text{s}}\right) \\ w_{\max} &= \frac{\pi}{2} \left(\frac{\text{rad}}{\text{s}}\right). \end{aligned}$$

The control signal constraints for the eight-shaped curve are selected as follows:

$$\begin{aligned} v_{\max} &= 0.3 \left(\frac{\text{m}}{\text{s}}\right) \\ w_{\max} &= 0.5 \left(\frac{\text{rad}}{\text{s}}\right). \end{aligned}$$

The maximum number of the optimization steps is selected as 5. The larger the maximum number of the optimization step, the better the tracking performance; however, the more time the computation will take. The control horizon T and the control time interval δ are selected based on the tracking trajectories. Due to the adding of the terminal-state region constraint, T should be long enough to guarantee the terminal state moving into the terminal-state region. This value can be found offline through a trail and error approach. δ should not be selected as being very small because the optimization algorithm takes time at each step. $T = 5$ s and $\delta = 0.5$ s are used. The number of the predictive steps is therefore 10. The model simulation time is selected as 0.1 s.

VI. SIMULATION RESULTS

The simulations were tested on a PC. An initial pose was selected for the circle test: $(1, -0.2, \pi/2)$. The tracking results are shown in Fig. 1, including (a) the trajectories, (b) the control signals, and (c) the error states. The tracking trajectory finally converged to the reference circle, the control signals converged to the reference control signals, and the error state converged to zero. The control signals did not go beyond their limitations.

The initial pose selected for the eight-shaped curve tracking test is $(-0.5, 0, \pi/3)$. The tracking results are shown in Fig. 2, including (a) the trajectories, (b) the control signals, and (c) the

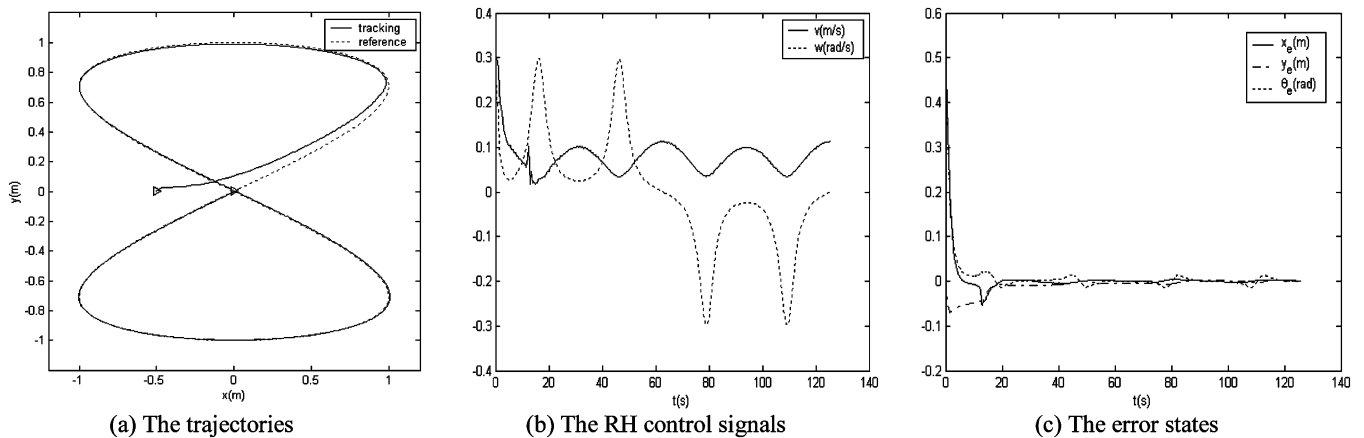


Fig. 2. Eight-shaped curve tracking.

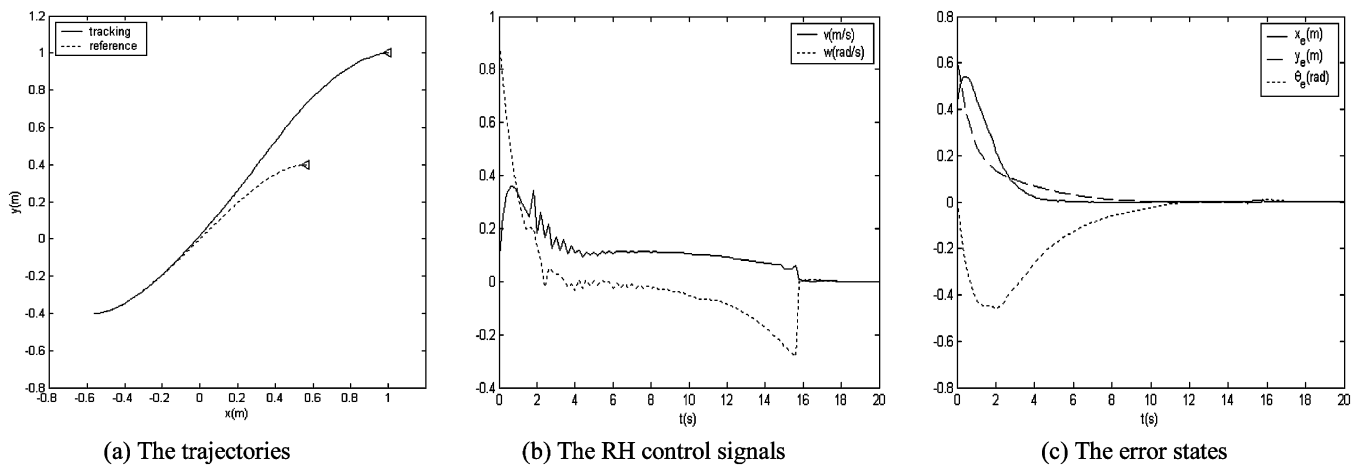


Fig. 3. Parallel parking line tracking.

error states. Although the speeds and states had errors at the beginning of the tracking, finally the robot trajectory converged to the reference curve, the control signals converged to the reference control signals, and the error state converged to zero.

A test was conducted with an initial pose $(1, 1, \pi)$ for the parallel parking line-tracking test. The tracking results are shown in Fig. 3, including (a) the trajectories, (b) the control signals, and (c) the error states. These results show that the robot can track the parallel parking line and stop at the final pose. At $t \approx 16$ s, the RH controller regulated the robot to reduce the error states [see the small changes of the control signals in Fig. 3(b)], and the errors converged to zero.

The variations of the control signals were caused by the sub-optimal solution. They can be smoothed out by increasing the optimization time or increasing the weight parameters R .

VII. CONCLUSION

This paper presents a stabilizing RH controller for the tracking control of nonholonomic mobile robots. A terminal-state region and its corresponding local controller are developed to guarantee the stability of controlled systems. The proposed RH controller can be used for simultaneous tracking control and regulation problems.

The computation is one of the problems to use RH controllers in real-time systems. How to improve the computation efficiency is still under investigation. The proposed RH controller needs an initial feasible solution. Currently, a trial-and-error approach is used. Feasibility analysis of initial solutions is one of our future works.

REFERENCES

- [1] R. P. Bitmead, M. Gevers, and V. Wertz, *Adaptive Optimal Control: The Thinking Man's GPC*. Englewood Cliffs, NJ: Prentice-Hall, 1990.
- [2] A. M. Bloch and S. Drakunov, "Tracking in nonholonomic dynamic systems via sliding modes," in *Proc. 34th IEEE CDC*, New Orleans, LA, 1995, pp. 2103–2106.
- [3] R. W. Brockett, "Asymptotic stability and feedback stabilization," *Differential Geometry Control Theory*, pp. 181–191, 1983.
- [4] C. de Wit and O. J. Sordalen, "Exponential stabilization of mobile robots with nonholonomic constraints," *IEEE Trans. Autom. Control*, vol. 37, no. 11, pp. 1791–1797, Nov. 1992.
- [5] H. Chen and F. Allgower, "A quasi-infinite horizon nonlinear model predictive control scheme with guaranteed stability," *Automatica*, vol. 34, no. 10, pp. 1205–1217, 1998.
- [6] A. De Luca and M. D. Di Benedetto, "Control of nonholonomic systems via dynamic compensation," *Kybernetika*, vol. 29, no. 6, pp. 593–608, 1993.
- [7] G. De Nicolao, L. Magni, and R. Scattolini, "Stabilizing receding-horizon control of nonlinear time varying systems," *IEEE Trans. Autom. Control*, vol. 43, no. 7, pp. 1030–1036, Jul. 1998.

- [8] W. E. Dixon, D. M. Dawson, F. Zhang, and E. Zergeroglu, "Global exponential tracking control of a mobile robot system via a PE condition," *IEEE Trans. Syst., Man, Cybern. B, Cybern.*, vol. 30, no. 1, pp. 129–142, Feb. 2000.
- [9] B. d'Andrea-Novell, G. Campion, and G. Bastin, "Control of nonholonomic wheeled mobile robots by state feedback linearization," *Int. J. Robot. Res.*, vol. 14, no. 6, pp. 543–559, 1995.
- [10] R. Fierro and F. L. Lewis, "Control of a nonholonomic mobile robot: Backstepping kinematics into dynamics," in *Proc. 34th IEEE CDC*, New Orleans, LA, 1995, pp. 3805–3810.
- [11] F. A. C. C. Fontes, "A general framework to design stabilizing nonlinear model predictive controllers," *Syst. Control Lett.*, vol. 42, no. 2, pp. 127–143, 2001.
- [12] —, "Discontinuous feedbacks, discontinuous optimal controls and continuous-time model predictive control," *Int. J. Robust Nonlinear Control*, vol. 13, no. 3–4, pp. 191–209, 2003.
- [13] G. Indiveri, "Kinematic time-invariant control of a 2-D nonholonomic vehicle," in *Proc. 38th IEEE CDC*, 1999, pp. 2112–2117.
- [14] A. Jadbabaie, J. Yu, and J. Hauser, "Stabilizing receding horizon control of nonlinear systems: A control Lyapunov function approach," in *Proc. Amer. Control Conf.*, San Diego, CA, 1999, pp. 1535–1539.
- [15] Z. P. Jinag and H. Nijmeijer, "Tracking control of mobile robots: A case study in backstepping," *Automatica*, vol. 33, pp. 1393–1399, 1997.
- [16] Y. J. Kanayama, Y. Kimura, F. Miyazaki, and T. Noguchi, "A stable tracking control method for an autonomous mobile robot," in *Proc. IEEE Int. Conf. Robot. Autom.*, 1990, pp. 384–389.
- [17] S. S. Keerthi and E. G. Gilbert, "Optimal infinite-horizon feedback laws for a general class of constrained discrete-time systems: Stability and moving-horizon approximations," *J. Optim. Theory Appl.*, vol. 57, pp. 265–293, 1988.
- [18] T. C. Lee, K. T. Sun, C. H. Lee, and C. C. Teng, "Tracking control of unicycle-modeled mobile robots using a saturation feedback controller," *IEEE Trans. Control Syst. Technol.*, vol. 9, no. 2, pp. 305–318, Mar. 2001.
- [19] D. Q. Mayne, J. B. Rawlings, C. V. Rao, and P. O. M. Scokaert, "Constrained model predictive control: Stability and optimality," *Automatica*, vol. 36, pp. 789–814, 2000.
- [20] G. Oriolo, A. De Luca, and M. Vendittelli, "WMR control via dynamic feedback linearization: Design, implementation, and experimental validation," *IEEE Trans. Control Syst. Technol.*, vol. 10, no. 6, pp. 835–852, Nov. 2002.
- [21] J. Pomet, "Explicit design of time-varying stabilizing control laws for a class of controllable systems without drift," *Syst. Control Lett.*, vol. 18, no. 2, pp. 147–158, 1992.
- [22] J. Primbs, V. Nevistic, and J. Doyle, "A receding horizon generalization of pointwise min-norm controllers," *IEEE Trans. Autom. Control*, vol. 45, no. 5, pp. 898–909, May 2000.
- [23] J. B. Rawlings and K. R. Muske, "Stability of constrained receding horizon control," *IEEE Trans. Autom. Control*, vol. 38, no. 10, pp. 1512–1516, Oct. 1993.
- [24] C. Samson and K. Ait-Abderrahim, "Feedback control of a nonholonomic wheeled cart in Cartesian space," in *Proc. IEEE Int. Conf. Robot. Autom.*, 1991, pp. 1136–1141.
- [25] P. O. M. Scokaert, D. Q. Mayne, and J. B. Rawlings, "Suboptimal model predictive control (feasibility implies stability)," *IEEE Trans. Autom. Control*, vol. 44, pp. 648–654, 1999.
- [26] J. E. Slotine and W. Li, *Applied Nonlinear Control*. Englewood Cliffs, NJ: Prentice-Hall, 1991.
- [27] A. Teel, R. Murray, and C. Walsh, "Nonholonomic control systems: From steering to stabilization with sinusoids," *Int. J. Control*, vol. 62, no. 4, pp. 849–870, 1995.
- [28] H. Van Essen and H. Nijmeijer, "Nonlinear model predictive control of constrained mobile robot," in *Proc. Eur. Control Conf.*, 2001, pp. 1157–1162.